Monika Andrych-Zalewska, Łukasz Wielki, Krzysztof Ziora

CFD analysis of the Ferrari 348 GTC intake system

JEL: L62 DOI: 10.24136/atest.2019.138
Data zgłoszenia: 05.04.2019 Data akceptacji: 26.06.2019

The article presents CFD (Computational Fluid Dynamics) analysis of the intake system of a Ferrari 348 GTC sports car. With this system, an adequate amount of air is supplied relative to the current demand for fuel combustion. The air demand of a given engine was deter-mined, then analyzes were carried out. The article contains an analy-sis of the velocity distribution: total velocities, angular velocities and static pressure distribution. In addition, local velocity and flow in the filtration chamber were determined along with the flow directions and returns as well as power lines. The cycle impact on the temperature, locations of the highest speed drop, increase in turbulence, the largest pressure differences, and modulus of elasticity were determined. This information allows to assess whether there are no unwanted phe-nomena occurring in the system, such as flow disturbances. The Ansys Fluent software was used for analysis.

Keywords: intake system, CFD analysis, internal combustion engine, modeling, flow, Ansys.

Introduction

Modern spark-ignition engines must be characterized by large volumetric power indicators, which makes it possible to obtain engines with small mass. This result can be achieved by increasing the rotational speed and the engine volumetric efficiency [5].

Regarding the volumetric efficiency improvement, the following development tendencies are observed: optimization of intake systems (along with increasing the number of valves) and the use of controlled dynamic and compressor charging (mainly turbocompressor). The increase of the cylinders volumetric efficiency with a fresh air and fuel mixture requires a detailed knowledge and mapping of phenomena occurring in its intake system, including the process of filling the cylinder with the gases taking into account the gas behavior during its movement in the above system and laws governing this process. This is extremely important not only from the point of view of improving the volumetric conditions and as a consequence of the combustion process in the engine, and thus also the reduction of exhaust emissions [8].

In addition, it is important to maintain the smallest possible differences in the volumetric efficiency between individual cylinders and the smallest possible discrepancies in the excess air coefficient. This requires special intake system solutions with carefully selected shapes. The system includes an air filter. It must be very effective at low pressure drops. The next element is the inlet manifold, often made of aluminum or usually made of plastic. In order to achieve low flow resistance, the filter surface area is usually increased, which leads to the expansion of the filter external dimensions.

In principle, each contemporary intake system in a spark-ignition engine, in addition to the previously mentioned functions, introduce the dynamic recharging effect, resulting from the vibrations of the column flowing to the cylinder [5]. The wave theory is related to constantly occurring pressure disturbances that create standing waves in the inlet pipe. Pressure disturbances result from cyclical engine operation due to suction. In the case when the amplitude of the initial pulse is large and the attenuation of the wave is small, the standing wave influences the pressure in the free passage of the valve and thus the volumetric efficiency [7, 9].

The article presents CFD (Computational Fluid Dynamics) analysis of the Ferrari 348 GTC (fig. 1) intake system (fig. 2) [6] aimed at familiarizing with the flowing medium velocity distribution and its pressure value. This information allows to assess whether there are no adverse phenomena in the system, such as flow disturbances.

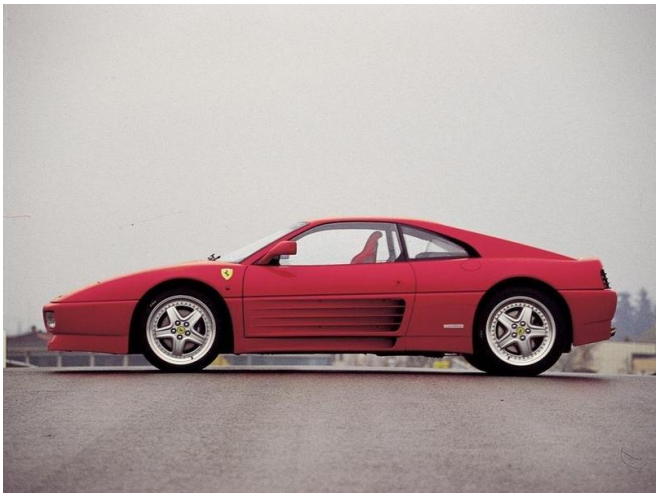

Fig. 1. Ferrari 348 GTC [6, 18]

Fig. 2. Ferrari 348 GTC intake system [31]

By discretization and numerical solution of partial differential equations describing the flow, it is possible to determine the distribution of velocity, pressure, temperature and other parameters in the flow. Modern CFD programs enable solving flows with regard to viscosity and compressibility, multiphase flows, flows in which chemical reactions or combustion processes occur, flows through porous structures, and flows in which the medium is Newtonian or non-Newtonian fluid. It is possible to simulate the interaction between liquid and solid. Most CFD programs are based on Navier-Stokes equations (mass, momentum and energy equation for fluid) and discretize them using finite volume methods, finite element methods or finite difference methods [13, 14, 27].

Each CFD calculation program based on the RANS technique has the ability to run and select one of the existing turbulence models.

1.Calculation part

In order to simulate the flow of the medium in the intake manifold, calculations of the necessary parameters were made, assuming that the intake system was running for the vehicle at maximum speed, i.e. with full engine load (full power characteristic).

The flow velocity was first determined:

The following parameters and operating conditions of the engine were adopted [1, 10, 11]:

- rotation speed n = 8000 rpm,
- displacement V_{ss} = 3.4 dm^3,
- power P = 281000 W (382 KM),
- volumetric efficiency η_v = 0.9,
- diameter of the flow cross-section d = 0.06 m,

$$Q = \frac{n}{2} \bullet \eta_v \bullet V_{ss} \tag{1}$$

$$Q = 0.2 \frac{m^3}{s}$$

$$Q = 2 \frac{\pi d^2}{4} \bullet V \tag{2}$$

$$V = \frac{2Q}{\pi d^2} = 36.09 \frac{m}{s}$$

where: Q [m^3/s] – engine air demand,
V [m/s] – air flow speed.

The next step in the calculation part was to determine flow parameters.

An indispensable criterion is the number Reynolds, whose critical value allows to determine the critical state flow separating the area of static laminar flow from turbulent flow. Loss of laminar flow stability and the transition to the form of turbulent flow occurs in the effect of an excessive increase in inertia forces over the forces of viscosity, acting on moving elements. In the Anglo-Saxon literature, Reynolds equation as modified Navier - Stokes equations, adapted to the description turbulent flows are called Reynolds Avaraged Navier - Stokes Equations, abbreviated as RANS. Classic turbulence modeling is based on the Reynolds hypothesis according to which, temporary values of all those characterizing the flow of physical quantities at a given point of the flow area are the sum of the values time-averaged and component of fluctuations (turbulence), which is a random function of time and space. [28].

Calculation of the Reynolds number Re

- Kinematic viscosity for air at temperature 200ºC: $\nu = 35 \bullet 10^{-6}$ m^2/s

$$Re = \frac{V \bullet d}{\nu} \tag{3}$$

$$Re = \frac{36.09 \bullet 0{,}06}{35 \bullet 10^{-6}} = 61874.43$$

2. Flow simulation

The preparation of a simulation model using ANSYS software consisted of the following steps [30]:

- geometry preparation in CAD environment,
- geometry importing into the Geometry module,
- computational grid generation in Mesh module,
- assumption of the initial and boundary conditions,
- carrying out simulations of the heat flow,
- analysis of results.

The projection of the intake system model (fig. 3) and its analysis was carried out in the Ansys Fluent program.

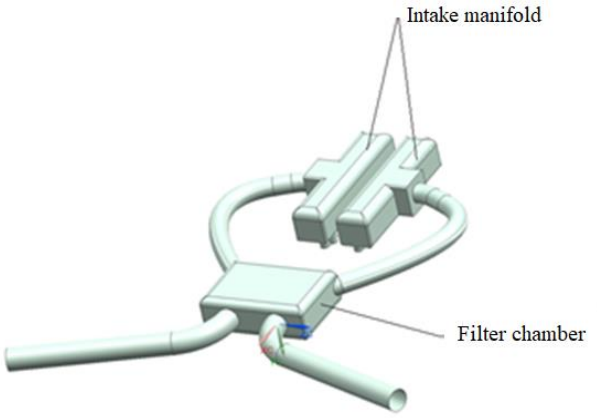

Fig. 3. Ferrari 348 GTC intake system model

After modeling the intake system construction, the mesh was created (fig. 4). Correct preparation of the grid requires compliance with the rules [19, 20, 21, 22]. Establishment of boundary and initial conditions and selection of other calculation parameters [19, 20, 23, 25]. The smallest element size must be smaller than the smallest linear dimension or features such as openings [13]. In this case, the smallest dimension has the diameter of the intake manifold end holes, which is 25 mm. Suggesting the recommendations of the FEA analysis program for the automatic selection of the mesh size [14]:

$$\delta < 0.5 \bullet A_{min} \tag{4}$$

where: δ [mm] – the length of the element parameter,
A_{min} [mm^2] – minimum surface,

and considering the cross-sectional area of the intake manifold end amounting to approximately 250 mm^2, the element size of 10 mm was selected. A wall effect has been defined using the program function. The flow direction of the medium (air) is shown in figure 5.

Parameters of the medium flowing in the tested intake manifold were determined - air with temperature and viscosity at atmospheric conditions:

- air density ρ =1.2 kg/m^3,
- kinematic viscosity ν = 35 • 10^{-6} m^2/s,
- dynamic viscosity μ = 42 •·10^{-6} kg/(m • s),
- air mass flow 1kg/s,
- air flow speed V = 36.09 m/s.

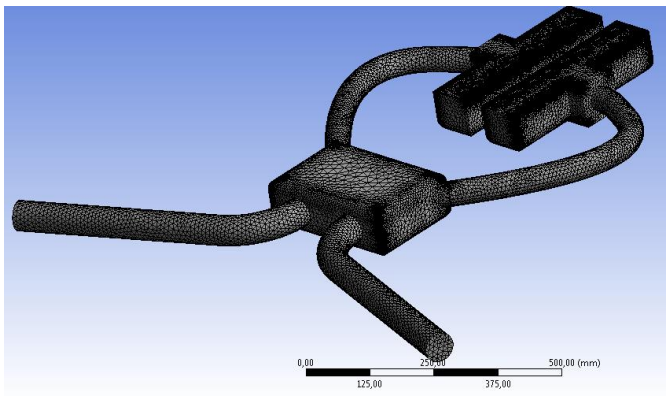

Fig. 4. Mesh model

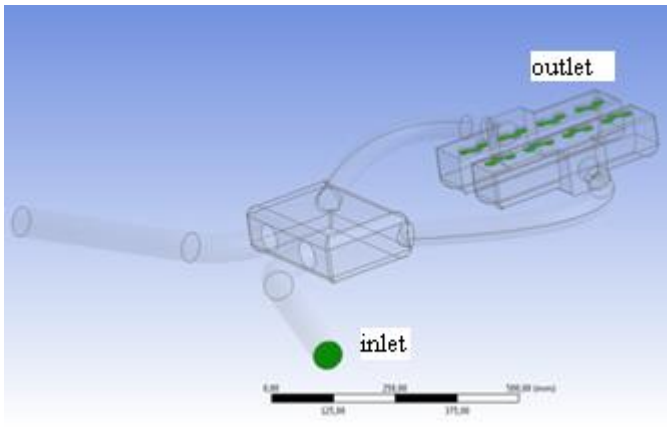

Fig. 5. Marking the medium flow entry and exit

Determining the boundary conditions:

The air velocity at the beginning of the system was assumed to be V_p = 0 m/s. The additional "charging" effect of the vehicle speed is compensated by the removal of the air filter element from the filter housing and by the adoption of a high volumetric efficiency η_v. Considering the calculated air demand of the engine, the final air velocity in the system was defined at V = 36.09 m/s.

The intensity of turbulence was chosen [2]: 10%.

To select the flow calculation model, a comparison was made (table 1) of the models available in the Ansys Fluent program (fig. 6)

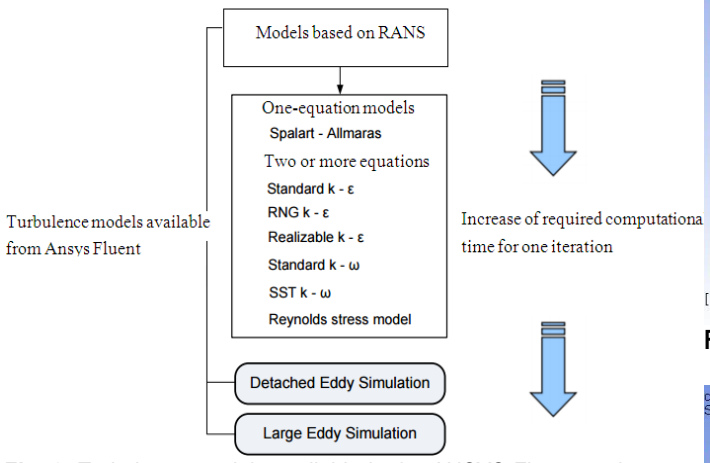

Fig. 6. Turbulence models available in the ANSYS Fluent package [28]

Tab. 1. Comparison of flow calculation models [17]

k-epsilon	k- omega	k- omega SST
k- kinetic energy of turbulence		
ε - the scale of turbulence (dissipation)	ω - k/ε (vorticity)	Combination of models k- ε and k- ω
The flow is fully turbulent	Laminar- turbulent flow	Laminar- turbulent flow

The k-omega SST model was chosen for flow simulation, since k-epsilon is not able to capture the appropriate turbulent behavior of the boundary layer until it is detached [16]. The SST turbulence model k - ω is a two-equation model hybrid. It is a smooth transition from the k-omega standard model, used in the boundary layer, for the model k-ε as far as moving away from the surface that limits flow. Contains modified formulation of turbulent viscosity for the purpose taking into account the effect of transport of main shear stresses.

The air temperature at the inlet to the intake system was assumed as T_1 = 293 K.

Using the Euler number Eu = 2.72 [12], the pressure difference was calculated Δp [Pa]:

$$Eu = \frac{\Delta p}{\rho V^2} \tag{5}$$

$$\Delta p = Eu \bullet \rho \bullet V^2 = 4251.32 \text{ Pa}$$

Pressure in the intake system was assumed at 0.85 • 10^5 Pa.

3. Simulation results

3.1. Simulation results of processes occurring in the intake manifold

Through the simulation of the flow in the Ansys Fluent program, the total velocity distribution was determined (fig. 7), as well as the static pressure distribution (fig. 8), and the angular velocity distribution (fig. 9).

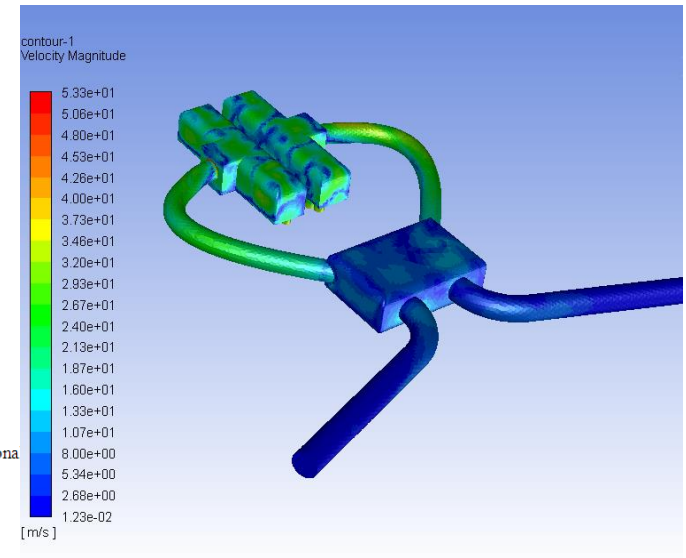

Fig. 7. Distribution of total speed values (Velocity Magnitude)

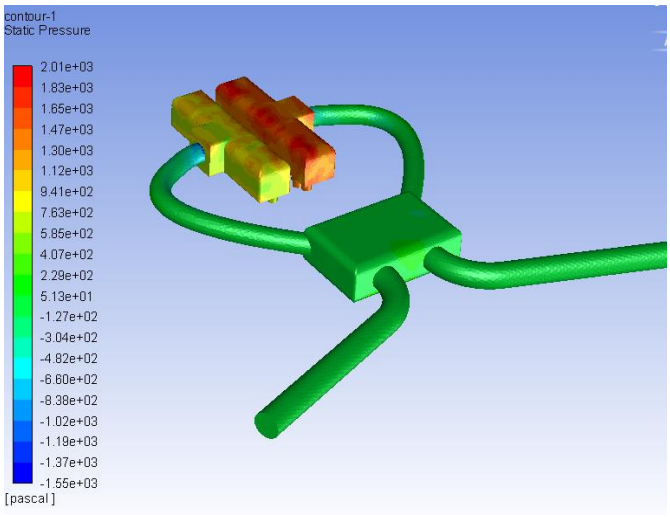

Fig. 8. Static pressure distribution

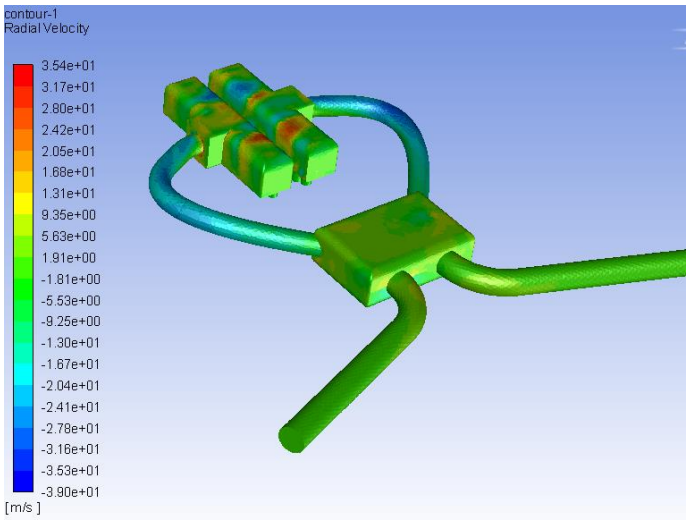

Fig. 9. Radial velocity distribution

3.2.Flow analysis in the filtration chamber

Determination of velocity vectors in the filtration chamber

The velocity distribution in the filtering chamber was determined without filter due to the lack of data on the filtering material (inertial resistance [1/m] and viscous resistance [1/m^2]). These are values determined experimentally.

Coefficient C: "inertial resistance" is determined by the formula [15]:

$$C = \frac{2\Delta pf}{\rho \bullet \Delta n} \tag{6}$$

where: C [1/m] – coefficient of inertial resistance,
Δn [mm] – thickness of the porous layer,
Δpf [P] – pressure drop in the filter.

To calculate this value, a pressure drop value in the filter Δpf is needed, which is unknown.

The viscous resistance factor is determined by the formula [15]:

$$\frac{1}{\alpha} = \frac{x}{\Delta n \bullet \mu} \tag{7}$$

where: $\frac{1}{\alpha}$ – [1/m^2] – viscous resistance coefficient,
x – coefficient of polynomial at the first velocity power for the pressure change equation from velocity change,
μ [kg/(m*s)] – dynamic air viscosity.

The XZ plane with dimensions of 200x385 mm and coordinates X = -100 mm, Y = 0 mm, Z = 70 mm was created.

Velocity and directions of velocity vectors over the entire chamber area were determined (fig.11). Data for creating velocity vectors is shown in the figure 10.

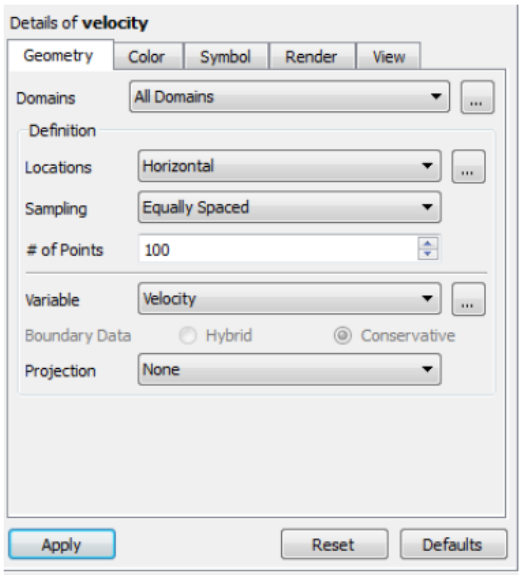

Fig. 10. Data for creating velocity vectors

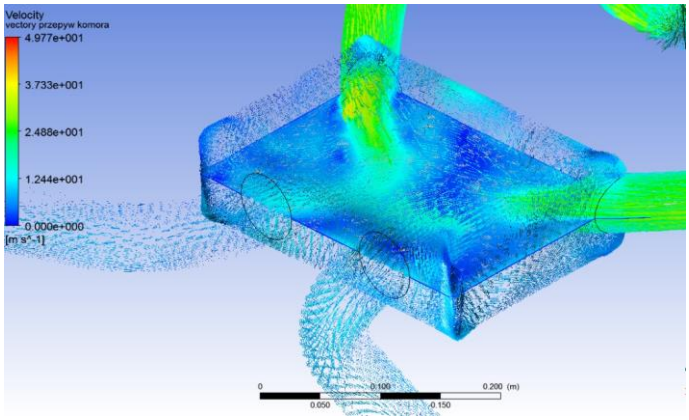

Fig. 11. Presentation of speed and directions of velocity vectors

Determination of 3D flow lines (fig. 11)

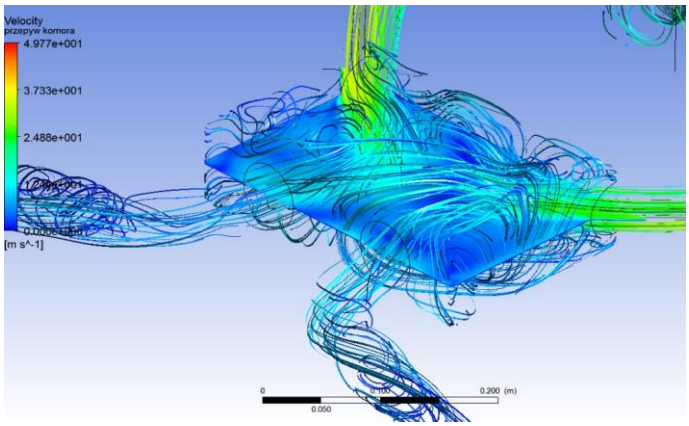

Fig. 12. Flow lines between the inflow and outflow of the medium in the filter chamber

Conclusions

In CFD methods, the problem is the interpretation of results, because the computer "counts everything ", unfortunately not always in accordance with the physical characteristics of the phenomenon. This requires a skilful interpretation of the results [27].

Based on the CFD (Computational Fluid Dynamics) analysis of a Ferrari 348 sports car intake system, the following conclusions are presented:

– The cycle impact on temperature

Based on the Sabathe cycle, the air required for the isobaric burning of the supplied fuel dose can be determined. From Gay-Lusac's law, it can be read that with a constantly increasing gas volume, the temperature increases proportionally [1].

– Highest velocity drop locations

Figure 7 indicates that this case can be found on the final section, due to the large difference in speed between the inflow and the outflow. The difference of paths to be covered by the air on the opposite sides of the pipe leads to an increase in turbulence, and hence to an increase in flow resistance. These turbulences cause large differences in gas velocity, which results in increased friction between air molecules and increased air temperature.

– Increase in turbulence - sudden change in the flow cross-section

This case occurs between the first tube and the filtration chamber. From fig. 9 it was found that there is a change in the angular velocity vector of the air mass, which means a change in the direction of the air turbulence. Due to the bent end of the first section of the pipe, turbulence is introduced, which then has to change the direction of rotation. In fig. 7, there is a large change in velocity for the space between these zones, resulting in reduced flow and pressure changes. These losses can be reduced by inserting a straight pipe section. Based on this analysis, the need to use a filter insert to reduce the Reynolds number can be seen, in order to change the flow type and reduce turbulence.

– Largest pressure differences location, modulus of elasticity

On the first section of the pipe connecting to the filtration chamber, the largest part has the greatest resistance, because the overpressure changes by an order of magnitude. This is due to the pressure drop with the local resistance, which is described by the presented formula, this means that the transitions should be as small as possible with the cross-section. In addition, the pressure drop can be seen in the air compressibility. The compressibility [3] depends on the pressure difference during compression, initial volume and modulus of longitudinal elasticity of the air. This restriction should be reduced by shortening the length of this section of pipe. The influence of the elasticity during intake can be found in fig. 8, because for the greater distance between the end of the system and the collector pipe and with the same pressure differences other flows occur. The longer path leads to a greater force needed to move a larger number of air molecules, the additional effect of inertia forces and increase the distance between them – the elastic modulus [4].

– There are locations in the filtering chamber where velocity vectors change their direction (fig. 11). Such places occur near the front and rear walls in the middle of the filter chamber, as well as the top and bottom walls, which can be seen by the flow lines (fig. 12). The flow line changes its course through a sudden pressure change. This leads to a change in accelerations and the emergence of mass forces. The increase in mass forces causes a drop in overpressure.

– Expanding the knowledge of complex flow mechanisms can be achieved through appropriate experimental verification of numerical models. The confrontation of simulation results with data obtained in industrial conditions is extremely difficult and often only possible for global parameters. Therefore, it is necessary to create experimental models with well-defined flow parameters.

List of markings

A_{min} [mm^2] – minimum surface
C [1/m] – coefficient of inertial resistance
d [m] – diameter of the flow cross-section
Eu [-] – Euler number
k – kinetic energy
n [rpm] – rotation speed
P [W] – engine power
Q [m^3/s] – engine air demand
Re [-] – Reynolds number
T_1 [K] – air temperature at the inlet to the intake system
V [m/s] – air flow speed
V_p – air speed at the beginning of the intake system
Vss [dm^3] – engine stroke
x [-] – polynomial coefficient
δ [mm] – the length of the element parameter
Δn [mm] – thickness of the porous layer
Δp [Pa] – differential pressure
Δpf [Pa] – pressure drop in the filter
ε – the scale of turbulence (dissipation)
η_v – volumetric efficiency
μ [kg/(m•s)] – dynamic viscosity
ν [m^2/s] – kinematic viscosity
ρ [kg/m^3] – air density
ω – k/ε vorticity
$\frac{1}{\alpha}$ [1/m^2] – viscous resistance coefficient

Bibliography:

1. P. Zając, L. M. Kołodziejczyk, Silniki spalinowe, WSiP, Warszawa 2001
2. ANSYS-Fluent-Tutorial-Guide_r170.pdf
3. S. Stryczek, Napęd hydrostatyczny T. 1 Elementy, WNT, Warszawa 2005
4. J. Mączyński, Mechanika płynów, PWN, Warszawa, 1966
5. S. Luft, Podstawy budowy silników, WKŁ, Warszawa2003
6. https://auto.ferrari.com/en_EN/sports-cars-models/past-models/348-gt-competizione/
7. K. Święcicki, Konstrukcja układu dolotowego silnika spalinowego, Modelowanie Inżynierskie nr 57, ISSN 1896-771X
8. J. Merkisz, J. Pielecha, S. Radzimirski, Emisja zanieczyszczeń motoryzacyjnych, WKŁ, Warszawa 2012
9. King F.R.B.: The inertia theory of engine breathing. "Automobil" 1968, No. 3-5.
10. https://autokult.pl/t/50447,ferrari-348, 12.01.2019 r.
11. http://zss.lublin.eu/wp-content/uploads/2016/09/2.5-Proces-spalania.pdf, 12.01.2019 r.
12. Jan A. Wajand, Jan T. Wajand Tłokowe silniki spalinowe średnio- i szybkoobrotowe, WNT, Warszawa, 2003.
13. ANSYS Meshing User's Guide_r130.pdf.
14. https://docs.plm.automation.siemens.com/tdoc/nx/10/nx_help#uid:id627236. 13.01.2019
15. https://www.sharcnet.ca/Software/Ansys/17.0/en-us/help/flu_ug/flu_ug_sec_bc_porous_ media.html 13.01.2019
16. FLUENT User's Guide
17. W. Bakuniak, Diploma Engineering: Symulacje przepływowe kolektora dolotowego dla bolidu Formuła Student , Poznań, 2015
18. https://www.topspeed.com/cars/ferrari/1994-ferrari-348-gt-competizione-ar79874.html
19. Ansys. www.ansys.com 2006.
20. 2. Atkins W.S., Consultants and Members of the NSC, Best Practice Guidelines for Marine Aplications of Computational Fluid Dynamics. Sirehna, HSVA, FLOWTECH, VTT, Imperial College of Science & Technology, Germanischer Lloyd, Astilleros Espanoles, http://pronet. wsatkins.co.uk/marnet/

21. Oertel Jr. H., Laurien E., Numerische Stromungsmechanik. Springer-Verlag, Berlin, 1995.
22. Olsen N., Computational Fluid Dynamics in Hydraulic and Sedimentation Engineering. The Norwegian University of Science and Technology, Trondheim, 1999.
23. Peyreat R., Taylor T., Computational Methods for Fluid Flow. Springer-Verlag, New York, 1983.
24. Rusiński E., Zasady Projektowania Konstrukcji Nośnych Pojazdów Samochodowych. Oficyna Wydawnicza Politechniki Wrocławskiej, Wrocław, 2002.
25. Thompson J., Warsi Z., Mastin C., Numerical Grid Generation Fundations and Applications. Elsavier Science Publishing Co., Inc., New York, 1985.
26. Wilcox D., Turbulence Modeling for CFD. KNI, Inc., Anaheim, 2002
27. Górniak A,, Michałowski R., Tkaczyk M., Symulacje układu dolotowego silnika zasilanego CNG, Autobusy 12/2011
28. Peszko M., Łygas K., Współczesne metody modelowania przepływów turbulentnych w otoczeniu poruszającego się autobusu miejskiego, Autobusy 12/2016
29. Suchecki M., Wołosz K., Weryfikacja kodu CFD dla symulacji przepływu cieczy wokół pęku rur przy użyciu metody DPIV, XVI Krajowa Konferencja Mechaniki Płynów, Waplewo 2004
30. Biały M., Pietrykowski K., Tulwin T., Magryta P., CFD numerical simulation of the indirect cooling system of an internal combustion engine, Combustion Engines, 3/2017
31. www.automobilemag.com

Analiza CFD układu dolotowego Ferrari 348 GTC

Analiza CFD układu dolotowego Ferrari 348 GTCW artykule przedstawiono analizę CFD (Computational Fluid Dynamics) układu dolotowego samochodu sportowego Ferrari 348 GTC. W tym systemie dostarczana jest odpowiednia ilość powietrza w stosunku do bieżącego zapotrzebowania na spalanie paliwa. Określono zapotrzebowanie na powietrze dla danego silnika, a następnie przeprowadzono analizy. Artykuł zawiera analizę rozkładu prędkości: prędkości całkowite, prędkości kątowe i rozkład ciśnienia statycznego. Dodatkowo wyznaczono lokalną prędkość i przepływ w komorze filtracyjnej wraz z kierunkami przepływu i powrotami oraz liniami energetycznymi. Oceniono wpływ cyklu na temperaturę, lokalizację największego spadku prędkości, wzrost turbulencji, największe różnice ciśnień i moduł sprężystości. Informacje te pozwalają ocenić, czy w systemie nie występują niepożądane zjawiska, takie jak zakłócenia przepływu. Do analizy wykorzystano oprogramowanie Ansys Fluent.

Słowa kluczowe: układ dolotowy, analiza CFD, silnik spalinowy, modelowanie, przepływ, Ansys

Authors:
dr inż. **Monika Andrych-Zalewska-** Wrocław University of Science and Technology, Faculty of Mechanical Engineering, Division of Automotive Engineering,
Braci Gierymskich 164 street, 51-505 Wroclaw
e-mail: monika.andrych@pwr.edu.pl
phone: +48 713477918
inż. **Łukasz Wielki-** Wrocław University of Science and Technology, Faculty of Mechanical Engineering,
e-mail: lukaszwielki@gmail.com
inż. **Krzysztof Ziora-** Wrocław University of Science and Technology, Faculty of Mechanical Engineering,
e-mail: k01zorbo@gmail.com